Fine-scale drivers of extreme wildfire spread events in California

Michael J. Koontz[a,b,c,*], Amy DeCastro[d,e], Malcolm P. North[f,g], Jennifer K. Balch[a,h], Andrew M. Latimer[f]

[a] *University of Colorado, Boulder, Cooperative Institute for Research in Environmental Sciences/Earth Lab, Boulder, CO, 80303*

[b] *United States Geological Survey, Fort Collins Science Center, Fort Collins, USA,*

[c] *Vibrant Planet, PBC, Incline Village, USA, 89451*

[d] *National Center for Atmospheric Research, Research Applications Laboratory, Boulder, CO, 80301*

[e] *Filsinger Engery Partners, Glendale, 80246*

[f] *University of California, Davis, Department of Plant Sciences, Davis, CA, 95616*

[g] *USDA Forest Service, Pacific Southwest Research Station, Mammoth Lakes, CA, 93546*

[h] *Environmental Data Science Innovation and Inclusion Lab, Boulder, CO, 80303*

Abstract

Fire behavior arises from the confluence of fuel, topography, weather, and human factors at multiple scales of time and space. Experimental burns under controlled conditions can help uncover the relative influence of these factors on fire propagation at fine temporal resolutions (e.g., over the course of minutes, hours, or days), but only at small spatial extents. On the other hand, characterizing phenomenological patterns across broad spatial extents can add to our understanding of wildfire, but only at coarser temporal resolutions (e.g., over the course of whole fires, fire seasons, years, or decades). Understanding fire phenomena at finer temporal resolutions across broad spatial extents simultaneously is challenging. Here, we investigate the fine-scale drivers of daily fire area of increase across the state of California over a two-decade period.

Keywords: wildfire, megafire, risk, hazard

1. Introduction

Over the past two decades, wildfires in California have significantly grown in size and severity, with major ecological and social impacts. Wildfire has reached sizes and daily spread rates that are much higher than those seen throughout most of the 20th century, posing a growing risk to communities in the wildland urban interface (WUI). These fires are spreading despite record fire suppression efforts and costs (reaching $4.4 billion in 2021 for Federal Suppression only [https://www.nifc.gov/fire-information/statistics/suppression-costs]).

Many fires escape containment and are simply spreading too fast and releasing too much energy to be fought effectively. Crucially, though large fires often burn for months, only a few days of extremely rapid spread generally account for most area burned, as well as most damage to property and lives lost (Balch et al., 2024). For example, in the record fire year of 2020, of the 4 million hectares burned in the United states, >50% burned in just the largest 5% of fire-days (Coop et al., 2022). To better understand the causes of

*Corresponding author
Email address: mkoontz@usgs.gov (Michael J. Koontz)

wildfire impacts and threats to communities, it's important to discover what drives these extreme spread events. While the term "megafires" is increasingly used to characterize the larger scale and intensity of some recent fires (Stephens et al., 2014; Tedim et al., 2018; Linley et al., 2022), we focus here on the few days of extreme spread during which these fires exert most of their dangerous and negative effects – we call these days of extremely fast fire spread "extreme wildfire events" (EWEs). Explaining these events requires a finer spatial and temporal analysis of fire spread than explaining variation in area burned.

Recent advances in mapping fire spread at a daily time step (Parks, 2014; Balch et al., 2020) and more recently a half-daily time step (Chen et al., 2022) have enabled research into drivers of fire behavior at finer time-scales over large areas. Previous research has found strong associations between the rate of fire spread, fire intensity, and fire severity (McFarland et al., 2025). Higher temperatures drive higher risk of extreme spread via higher aridity and lower fuel moisture, suggesting that extreme spread has increased and will continue to increase with anthropogenic climate warming (Brown et al., 2023). In this study, we complement these previous studies on drivers of extreme spread by taking a more comprehensive look at all classes of drivers including weather, fuel, topography, and human factors. In our analysis, we also consider where fire is already burning actively in an effort to identify factors that distinguish active and extreme spread.

[Placeholder for possible methods paragraph in intro] Relating potential drivers to daily burned area presents a methodological challenge, since the distributions of fine-grained spatial variables such as topographic and fuel variables are often scale-dependent. To address this scale challenge, we developed a new randomization method to attempt to normalize the driver values for burned areas of different sizes. Essentially, we compared the value of spatial drivers to the values for 500 polygons of the same size and shape, randomly placed throughout the target domain. This procedure normalized values effectively for many spatially varying drivers (see Methods). To characterize the associations between drivers and EWE risk in more detail, we then used random forest, which allowed us to evaluate the effect of each driver in context of the other driver variables. Following recent results in machine learning, we used unbiased methods to evaluate variable importance, measure model performance, and characterize the form of associations (see Methods).

In this study, we use daily time-step fire data to investigate drivers of extremely rapid spread in California from 2003-2020. We define extremely rapid spread as the top 5% of all spread days and term them "extreme wildfire events" (EWEs). We describe the spatial and temporal distribution of these events in California. We build on previous research that suggests rapid spread dynamics may be different in forests vs other Mediterranean-climate vegetation (woodland, scrubland, grassland) to investigate whether the predictors of rapid spread differ in important ways between these two zones. We also investigate whether the drivers of rapid spread differ at the beginning of a wildfire from later on during the event. To do this, we compile a large data set encompassing all major classes of drivers, including weather, fuels, topography, and human factors, including proxies for availability of firefighting resources and accessibility via roads. Specifically, we ask the following questions: 1. What are the drivers of EWEs, and what is the relative importance of different classes of drivers, including weather, fuels, topography, and human factors? ["t-tests", spatialRF analysis] 1. Are EWEs driven by different factors in different ecosystems with distinct fire regimes? In particular, conifer forests vs mediterranean shrublands ["t-tests", spatialRF analysis] 3. Is there a distinct set of factors associated with escape from containment and extremely rapid spread early on in the life of a wildfire (i.e., within the first week) compared to later on (i.e., after three weeks)? ["t-tests", spatialRF analysis of the early and small-size subsets of the data] 4. Finally, we use geographically varying drivers to produce a map ranking potential operational delineations (i.e., PODs (Thompson et al., 2022)) in California's Sierra Nevada forests, for propensity to support extreme fire spread. (compare to previous work Peeler et al., 2023, mapping risk).

2. Methods

3. Overview of FIRED dataset; defining "extreme spread event"

We used the FIRED algorithm with a spatial window of 5 pixels and a temporal window of 11 days (Balch et al., 2020) to generate a dataset of daily fire growth in California between 2003 and 2020. Each polygon represents the daily area of growth– a spread event– for one fire event. Across all daily polygons, we calculated the 95th percentile of daily area of growth and classified all spread events that exceeded that threshold (corresponding to spread > xxxx ha) as an "extreme spread event" (ESE). For each spread event, we assigned a Resolve biome based on greatest fractional coverage: 1) temperate conifer forests, 2) Mediterranean forests, woodlands, and scrub 3) temperate grasslands, savannas, and shrublands, and 4) deserts and xeric shrublands (Resolve 2017). To capture a semblance of "surprise" in the spread events, we divided events into two temporal contexts: "early" spread events occurred within the first seven days of the fire event, and "late" spread events occurred after the first seven days of the fire event. Ultimately, we assembled eight separate datasets (unique combinations of four biomes and two temporal contexts).

4. Assembling predictor variables

We collated a set of 50 potential predictor variables in five categories: human, weather, topography, fuel, and "fire" (which only included the daily area of increase of the most recent spread event within the same fire event). Table 1 provides the source and means of calculating each variable, and we expand on the description for more complicated derived variables here. We used Google Earth Engine to extract all weather and topography data (Gorelick et al., 2017). We also used Google Earth Engine to extract NDVI, NDVI heterogeneity, and landcover data from the USDA Forest Service's Landcover Change Monitoring System (in the fuel category). For each biome/temporal context, we removed all spread events that had missing data for any of the covariates. For modeling, we divided each of the datasets into 10 spatial folds based on the centroid location of the largest polygon in the spread event using the `spatialsample` package in R (Mahoney et al., 2023). We ensured that all predictor variables had greater than 0 variance in each spatial fold. We removed spatial folds that resulted in fewer than 40 observations or fewer than 2 extreme spread events.

4.1. Normalizing covariates as percentiles to characterize counterfactuals

To aid the comparisons of spread events across time and space, we normalized many predictor variables by converting the measured value of the predictor to a percentile. Some predictor variables were already measured in a way that codified their context (e.g., z-scores), and we did not further adjust these. We opted to not normalize predictor variables that were measured at very broad scales (i.e., number of concurrent fires, National Preparedness Level), when there wasn't a clear monotonicity to the measurements (i.e., predictors based on wind direction), or when normalization didn't enable a counterfactual comparison to "expected" conditions independent of fire (i.e., area of growth of previous spread event). See Table 1 for an accounting of the variables to which we made further normalization adjustments.

For each weather variable that was normalized, we generated a 401-layer raster at the data product's original resolution where each layer represented the value of that weather variable that corresponded to a particular percentile (0th through 100th percentiles in increments of 0.25) aggregated through time between January 1, 1981 and December 31, 2020. Then, for each daily fire polygon location, we matched the extracted weather variable value on the day of the fire to the value closest to it in the 401-layer raster. The percentile to which the layer of closest match corresponded was the approximate percentile of the observed fire weather on the day of interest (compared to the 40-year record of the weather data at that location).

For each normalized fuel and topography variable measurement in each spread event, we calculated their percentile within a sample of measurements taken of the same variable within polygons of the same size and shape of the spread event but over areas not in the actual location of the spread event (Figure 1). A priori, we determined approximately 500 "fire independent" locations within each biome based on a hexagonal grid. For each spread event, we created a copy of its polygon at each of those fire independent locations using a simple translation, such that its new centroid coincided with one of the fire independent points. We matched the biome of the fire independent locations with the biome of the whole fire event to which the spread event belonged. To avoid the fire independent polygons overlapping the ocean, we buffered the hexagonal grid 50km inward from the coast. Further, we calculated the fractional cover of water within each fire independent polygon, and used it as the denominator for calculating fractional cover of fire independent fuel and topography variables. We also excluded fire-independent polygons whose areal cover of water divided by the areal cover of water in the spread event was greater than 1.1.

4.2. Weather

For each daily polygon, we extracted the weather variables from the referenced data source at the spatial centroid of the daily polygon in the case of single-polygon geometries and from the spatial centroid of the largest polygon for multipolygon geometries. We extracted weather data derived from the ERA5-Land reanalysis for each of the 24 observations within the day that the spread event represented (Hersbach et al., 2020) and then summarized those values in various ways as described below to produce a single daily value. We produced mean and standard deviation daily summaries of wind direction using a sine transformation to capture the east/west axis (with a value of 1 representing wind from the east and a value of -1 representing wind from the west) and a cosine transformation to capture the north/south axis (with a value of 1 representing wind from the north and a value of 0 representing wind from the south). We summarized wind speed, relative humidity, vapor pressure deficit, and temperature percentiles as their minima and maxima for the day. GRIDMET variables on a daily scale were extracted for each daily polygon for the relevant day, and GRIDMET drought variables (all standardized precipitation evapotranspiration indices (SPEI) and the Palmer Drought Severity Index (PDSI)) were extracted for each spread event at the nearest 5-day interval of those data products.

4.3. Topography

We implemented the rumple index as "surface area / projected area" (Jenness, 2004) to capture terrain roughness across each daily polygon using the 3DEP 10m digital elevation model (USGS – citation needed). We simplified the fifteen different landform types from (Theobald et al., 2015) into five broader categories by combining some similar, relatively rare cover types (see Table 1), then calculated the fractional cover of each of the five broader categories for each daily polygon. We then calculated the Shannon-Wiener diversity index for landform cover using the fractional cover of those five landform types per daily polygon using the `vegan` package in R (Oksanen et al., 2025).

4.4. Fuels

We extracted the spatial mean NDVI across each daily polygon for the year prior to the observed fire spread. The NDVI data was derived from a temporal mean composite raster using Landsat data and the same image window as (Parks et al., 2019) for California (152nd to 258th day of year) after first masking snow, water, clouds, and cloud shadows. We also calculated the rumple index (Jenness, 2004) to the NDVI across each daily polygon to capture variability in vegetation cover across a broad area. We first multiplied NDVI (on a -1 to 1 scale) by 100 in order to avoid computational underflow errors. We aggregated the 14 categories of the "land cover" layer of the Landcover Monitoring Change System v2020-5 (USDA Forest Service– citation needed) into four simpler categories based on the earliest seral stage/lowest biomass growth form present in the categories that represent mixtures of physiognomic types (e.g., "shrub/tree mix" is grouped

with "shrubs" in a single "shrubs" category; see Table 1) and then calculated the fractional cover of those broader categories within each spread event. We also calculated the Shannon-Wiener diversity index for land cover using these four broader categories as we did for topographic landform. We characterized the fractional cover of 10-year fire and insect/disease disturbance histories using annual Landfire disturbance data. We subdivided the fire category into "high-severity" and "not high-severity" as well as "recent" (one- to five-year history) and "less recent" (six- to ten-year history).

4.5. Human

The number of fires burning concurrently – a proxy for demand on firefighting resources – was derived for each spread event using a subset of the FPA-FOD database (Short, 2022) based on events only in California and which had a reported start and end day. We assigned a National Preparedness Level to each spread event based on the day of burning (National Interagency Fire Center – citation needed; Cullen et al. (2020); Podschwit et al. (2020)). We calculated road density as "meters of road per hectare" within each spread event using data from CalTrans Functional Classification system (CalTrans <accessed 2022-12-20>). (Haight and and Fried, 2007) (Miller et al., 2012) (Safford et al., 2022) (CALFIRE, 2020)

4.6. Fire

To capture the effect of ignition pressure of the active fireline to cause spread into new areas, we included the area of growth from the previous spread event within the same fire event as a driver of daily area of growth. For the first spread event within a fire event, we recorded this value as zero.

5. Focus on temperate forest and Mediterranean forest, woodland, and scrub

Initial analysis revealed very little extreme spread events activity in the temperate grasslands and the xeric desert and shrub biomes, so we focused further analyses on the temperate forests and the Mediterranean forest, woodland, and scrub biomes.

6. Analysis of all spread events

We visualized the distribution and calculated the mean value of all predictor variables across the two remaining biomes and the two temporal contexts. For the normalized variables, we compared the mean normalized value to the expectation for the variable (i.e., 50th percentile or a z-score of 0) in order to characterize the overall conditions of fire spread, regardless of whether that spread was extreme or not.

7. Model predicting extreme spread events

7.1. Model tuning

For each of the two remaining biomes in two temporal contexts, we also built models that predicted whether or not a spread event was an extreme spread event in a random forest classification framework with probability forests (Malley et al., 2012) using the `ranger` package in R (Wright and Ziegler, 2017). This allowed for continuous predictions between 0 and 1, which allowed us to tune the classification threshold. We used a value of 1000 for the `num.trees` hyperparameter as a balance between computational needs and model skill (citation needed). We used class weights for the extreme spread events class as the reciprocal of the number of non-extreme spread events in the training data, and vice versa, in order to upsample the non-dominant class (citation needed). We used the `hellinger` split rule, which is more robust for classification

problems with unbalanced data (citation needed). We tuned the `mtry` (13 values), `sample.fraction` (6 values), and `min.node.size` (6 values) hyperparameters as well as the classification threshold (40 values) using a complete grid. We ran 10 iterations of each of the 10 spatial folds in order to account for the stochastic nature of building random forests. For each unique combination of `mtry`, `sample.fraction`, `min.node.size`, and classification threshold, we calculated the Matthew's Correlation Coefficient (MCC) across all 10 iterations and all 10 spatial folds (citations needed for MCC, Chicco and Poisot). For each model, we use the combination of hyperparameters that yields the highest mean MCC across spatial folds.

7.2. Variable importance

Conditional predictive impact

7.3. Response function interpretation

Accumulated local effects plots

8. Hazard mapping

- PODs
- How models used to predict relative hazard in different PODs under different assumptions about previous day's fireline length / area burned.

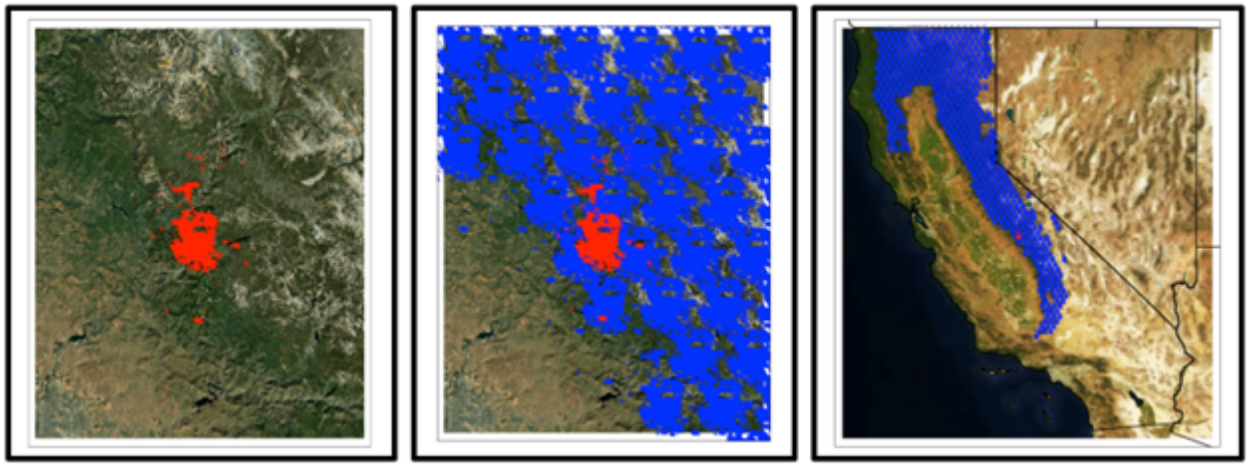

Figure 1: A) Location of the spread event on September 7, 2020 from the Creek Fire from the FIRED dataset. B) Location of actual spread event (red), and location of a portion of the fire-independent spread events (blue). C) Same as B, but showing coverage across the full temperate forest biome in the state of California.

9. Results

Figures 1. Conceptual diagram of fuel, topography, weather factors (and how they interact) to drive extreme wildfire events
1. Map of daily FIRED perimeter having active fire detections within it and delineation of fire head
1. Distribution of fireline intensity for all California fires 1. Distribution of multivariate fuel, topography, climate conditions 1.

Table 1. Akin to (Bowman et al., 2017) showing different categories of extreme wildfire events 1. Depending on how many are classified as "extreme", a table with the info joined from MTBS/FRAP

10. Discussion

- The hope for "let's manage fires for wildland benefit" will be fundamentally challenged by increasing megafire hazard with increasing number of concurrent fires
- Argues for need to set landscape up ahead of time
- Limitations of data (particularly wind)
- There is a natural cautiousness concerning fire management vs fire suppression since we don't have the workforce needed to manage several concurrent fires. This bolsters the argument for setting up the landscape for beneficial/ low severity fire ahead of time.

11. Acknowledgements

12. Author contributions

Author contributions are defined using the Contributor Roles Taxonomy (CRediT; https://casrai.org/credit/). Conceptualization: ; Data curation: ; Formal analysis: ; Funding acquisition: ; Investigation: ; Methodology: ; Project administration: ; Resources: ; Software: ; Supervision: ; Validation: ; Visualization: ; Writing – original draft: ; Writing – review and editing:

References

Balch, J.K., Iglesias, V., Mahood, A.L., Cook, M.C., Amaral, C., DeCastro, A., Leyk, S., McIntosh, T.L., Nagy, R.C., St. Denis, L., Tuff, T., Verleye, E., Williams, A.P., Kolden, C.A., 2024. The fastest-growing and most destructive fires in the US (2001 to 2020). Science 386, 425–431. doi:10.1126/science.adk5737.

Balch, J.K., St. Denis, L.A., Mahood, A.L., Mietkiewicz, N.P., Williams, T.M., McGlinchy, J., Cook, M.C., 2020. FIRED (Fire Events Delineation): An open, flexible algorithm and database of US fire events derived from the MODIS burned area product (2001–2019). Remote Sensing 12, 3498. doi:10.3390/rs12213498.

Bowman, D.M.J.S., Williamson, G.J., Abatzoglou, J.T., Kolden, C.A., Cochrane, M.A., Smith, A.M.S., 2017. Human exposure and sensitivity to globally extreme wildfire events. Nature Ecology & Evolution 1, 1–6. doi:10.1038/s41559-016-0058.

Brown, P.T., Hanley, H., Mahesh, A., Reed, C., Strenfel, S.J., Davis, S.J., Kochanski, A.K., Clements, C.B., 2023. Climate warming increases extreme daily wildfire growth risk in California. Nature , 1–7doi:10.1038/s41586-023-06444-3.

CALFIRE, 2020. 2020 Wildfire Siege.

Chen, Y., Hantson, S., Andela, N., Coffield, S.R., Graff, C.A., Morton, D.C., Ott, L.E., Foufoula-Georgiou, E., Smyth, P., Goulden, M.L., Randerson, J.T., 2022. California wildfire spread derived using VIIRS satellite observations and an object-based tracking system. Scientific Data 9, 249. doi:10.1038/s41597-022-01343-0.

Coop, J.D., Parks, S.A., Stevens-Rumann, C.S., Ritter, S.M., Hoffman, C.M., 2022. Extreme fire spread events and area burned under recent and future climate in the western USA. Global Ecology and Biogeography n/a. doi:10.1111/geb.13496.

Cullen, A.C., Axe, T., Podschwit, H., Cullen, A.C., Axe, T., Podschwit, H., 2020. High-severity wildfire potential – associating meteorology, climate, resource demand and wildfire activity with preparedness levels. International Journal of Wildland Fire 30, 30–41. doi:10.1071/WF20066.

Gorelick, N., Hancher, M., Dixon, M., Ilyushchenko, S., Thau, D., Moore, R., 2017. Google Earth Engine: Planetary-scale geospatial analysis for everyone. Remote Sensing of Environment 202, 18–27. doi:10.1016/j.rse.2017.06.031.

Haight, R.G., and Fried, J.S., 2007. Deploying Wildland Fire Suppression Resources with a Scenario-Based Standard Response Model. INFOR: Information Systems and Operational Research 45, 31–39. doi:10.3138/infor.45.1.31.

Hersbach, H., Bell, B., Berrisford, P., Hirahara, S., Horányi, A., Muñoz-Sabater, J., Nicolas, J., Peubey, C., Radu, R., Schepers, D., Simmons, A., Soci, C., Abdalla, S., Abellan, X., Balsamo, G., Bechtold, P., Biavati, G., Bidlot, J., Bonavita, M., De Chiara, G., Dahlgren, P., Dee, D., Diamantakis, M., Dragani, R., Flemming, J., Forbes, R., Fuentes, M., Geer, A., Haimberger, L., Healy, S., Hogan, R.J., Hólm, E., Janisková, M., Keeley, S., Laloyaux, P., Lopez, P., Lupu, C., Radnoti, G., de Rosnay, P., Rozum, I., Vamborg, F., Villaume, S., Thépaut, J.N., 2020. The ERA5 global reanalysis. Quarterly Journal of the Royal Meteorological Society 146, 1999–2049. doi:10.1002/qj.3803.

Jenness, J.S., 2004. Calculating landscape surface area from digital elevation models. Wildlife Society Bulletin 32 (3): 829-839 , 829–839.

Linley, G.D., Jolly, C.J., Doherty, T.S., Geary, W.L., Armenteras, D., Belcher, C.M., Bliege Bird, R., Duane, A., Fletcher, M.S., Giorgis, M.A., Haslem, A., Jones, G.M., Kelly, L.T., Lee, C.K.F., Nolan, R.H., Parr, C.L., Pausas, J.G., Price, J.N., Regos, A., Ritchie, E.G., Ruffault, J., Williamson, G.J., Wu, Q., Nimmo, D.G., 2022. What do you mean, 'megafire'? Global Ecology and Biogeography 31, 1906–1922. doi:10.1111/geb.13499.

Mahoney, M.J., Johnson, L.K., Silge, J., Frick, H., Kuhn, M., Beier, C.M., 2023. Assessing the performance of spatial cross-validation approaches for models of spatially structured data. doi:10.48550/arXiv.2303.07334, arXiv:2303.07334.

Malley, J.D., Kruppa, J., Dasgupta, A., Malley, K.G., Ziegler, A., 2012. Probability Machines. Methods of Information in Medicine 51, 74–81. doi:10.3414/ME00-01-0052.

McFarland, J.R., Coop, J.D., Balik, J.A., Rodman, K.C., Parks, S.A., Stevens-Rumann, C.S., 2025. Extreme Fire Spread Events Burn More Severely and Homogenize Postfire Landscapes in the Southwestern United States. Global Change Biology 31, e70106. doi:10.1111/gcb.70106.

Miller, J.D., Skinner, C.N., Safford, H.D., Knapp, E.E., Ramirez, C.M., 2012. Trends and causes of severity, size, and number of fires in northwestern California, USA. Ecological Applications 22, 184–203. doi:10.1890/10-2108.1.

Oksanen, J., Simpson, G.L., Blanchet, F.G., Kindt, R., Legendre, P., Minchin, P.R., O'Hara, R., Solymos, P., Stevens, M.H.H., Szoecs, E., Wagner, H., Barbour, M., Bedward, M., Bolker, B., Borcard, D., Carvalho, G., Chirico, M., De Caceres, M., Durand, S., Evangelista, H.B.A., FitzJohn, R., Friendly, M., Furneaux, B., Hannigan, G., Hill, M.O., Lahti, L., McGlinn, D., Ouellette, M.H., Ribeiro Cunha, E., Smith, T., Stier, A., Ter Braak, C.J., Weedon, J., Borman, T., 2025. Vegan: Community Ecology Package.

Parks, S.A., 2014. Mapping day-of-burning with coarse-resolution satellite fire-detection data. International Journal of Wildland Fire 23, 215–223. doi:10.1071/WF13138.

Parks, S.A., Holsinger, L.M., Koontz, M.J., Collins, L., Whitman, E., Parisien, M.A., Loehman, R.A., Barnes, J.L., Bourdon, J.F., Boucher, J., Boucher, Y., Caprio, A.C., Collingwood, A., Hall, R.J., Park, J., Saperstein, L.B., Smetanka, C., Smith, R.J., Soverel, N., 2019. Giving ecological meaning to satellite-derived fire severity metrics across North American forests. Remote Sensing 11, 1735. doi:10.3390/rs11141735.

Peeler, J.L., McCauley, L., Metlen, K.L., Woolley, T., Davis, K.T., Robles, M.D., Haugo, R.D., Riley, K.L., Higuera, P.E., Fargione, J.E., Addington, R.N., Bassett, S., Blankenship, K., Case, M.J., Chapman, T.B., Smith, E., Swaty, R., Welch, N., 2023. Identifying opportunity hot spots for reducing the risk of wildfire-caused carbon loss in western US conifer forests. Environmental Research Letters 18, 094040. doi:10.1088/1748-9326/acf05a.

Podschwit, H., Cullen, A., Podschwit, H., Cullen, A., 2020. Patterns and trends in simultaneous wildfire activity in the United States from 1984 to 2015. International Journal of Wildland Fire 29, 1057–1071. doi:10.1071/WF19150.

Safford, H.D., Paulson, A.K., Steel, Z.L., Young, D.J.N., Wayman, R.B., 2022. The 2020 California fire season: A year like no other, a return to the past or a harbinger of the future? Global Ecology and Biogeography 31, 2005–2025. doi:10.1111/geb.13498.

Short, K.C., 2022. Spatial wildfire occurrence data for the United States, 1992-2020. doi:10.2737/RDS-2013-0009.6.

Stephens, S.L., Burrows, N., Buyantuyev, A., Gray, R.W., Keane, R.E., Kubian, R., Liu, S., Seijo, F., Shu, L., Tolhurst, K.G., van Wagtendonk, J.W., 2014. Temperate and boreal forest mega-fires: Characteristics and challenges. Frontiers in Ecology and the Environment 12, 115–122. doi:10.1890/120332.

Tedim, F., Leone, V., Amraoui, M., Bouillon, C., Coughlan, M.R., Delogu, G.M., Fernandes, P.M., Ferreira, C., McCaffrey, S., McGee, T.K., Parente, J., Paton, D., Pereira, M.G., Ribeiro, L.M., Viegas, D.X., Xanthopoulos, G., 2018. Defining extreme wildfire events: Difficulties, challenges, and impacts. Fire 1, 9. doi:10.3390/fire1010009.

Theobald, D.M., Harrison-Atlas, D., Monahan, W.B., Albano, C.M., 2015. Ecologically-Relevant Maps of Landforms and Physiographic Diversity for Climate Adaptation Planning. PLOS ONE 10, e0143619. doi:10.1371/journal.pone.0143619.

Thompson, M.P., O'Connor, C.D., Gannon, B.M., Caggiano, M.D., Dunn, C.J., Schultz, C.A., Calkin, D.E., Pietruszka, B., Greiner, S.M., Stratton, R., Morisette, J.T., 2022. Potential operational delineations: New horizons for proactive, risk-informed strategic land and fire management. Fire Ecology 18, 17, s42408–022–00139–2. doi:10.1186/s42408-022-00139-2.

Wright, M.N., Ziegler, A., 2017. Ranger: A Fast Implementation of Random Forests for High Dimensional Data in C++ and R. Journal of Statistical Software 77, 1–17. doi:10.18637/jss.v077.i01.